Draft version December 4, 2017
Typeset using LaTeX **modern** style in AASTeX61

THE EFFECTS OF BINARITY ON PLANET OCCURRENCE RATES MEASURED BY TRANSIT SURVEYS

L. G. Bouma,[1] J. N. Winn,[1] and K. Masuda[1]

[1] *Department of Astrophysical Sciences, Princeton University, 4 Ivy Lane, Princeton, NJ 08540, USA*

Submitted to AAS journals.

ABSTRACT

This work aims to clarify the biases that stellar binarity introduces to occurrence rates inferred from transit surveys. In general, stellar multiplicity leads to diluted planetary radii, overestimated detection efficiencies, and an undercounted number of selected stars (but possibly an overcounted number of searched stars). These effects skew occurrence rate measurements in different directions, and we develop simple models that allow us to understand the crucial effects. For a model in which all stellar systems are either single or twin binaries, and all planets are identical, we find that ignoring binarity leads to an underestimate of the occurrence at the true radius by a multiplicative factor of 0.76 (assuming a 10% twin binary fraction). Using more realistic models for the stellar population and planetary radii, we find that ignoring binarity leads to a 10 - 30% underestimate of the number of planets per star, depending on the true radius distribution. For the occurrence of Earth-sized planets, in our most realistic model the rate is underestimated by $\approx 15\%$ – at present far smaller than systematic uncertainties on real $\eta_\oplus$ measurements. For hot Jupiters, we find that the inferred occurrence rate is $\approx 1.3\times$ smaller than the true rate around single stars. We suggest that this latter effect contributes to the discrepant hot Jupiter rates measured by *Kepler* and the California group's respective surveys.

Keywords: methods: data analysis — planets and satellites: detection — surveys

Corresponding author: L. Bouma
luke@astro.princeton.edu

1. INTRODUCTION

A group of astronomers wants to measure the mean number of planets of a certain type per star of a certain type. Ignoring stellar multiplicity, they perform a signal-to-noise limited transit survey, and detect a set of planets that appear to be of the desired class. They then choose the stars (among those initially surveyed) around which the planets of interest appeared to be searchable. Correcting for the geometric transit probability $p_{\rm tra}$, they report an apparent rate density,

$$\Gamma_{\rm a}(\mathcal{P}_{\rm a}, \mathcal{S}_{\rm a}) = \frac{N_{\rm det}(\mathcal{P}_{\rm a}, \mathcal{S}_{\rm a})}{N_{\rm s,a}(\mathcal{P}_{\rm a}, \mathcal{S}_{\rm a})} \times \frac{1}{p_{\rm tra}(\mathcal{P}_{\rm a}, \mathcal{S}_{\rm a})}. \quad (1)$$

where $\mathcal{P}_{\rm a}$, $\mathcal{S}_{\rm a}$ are the apparent planetary and stellar parameters, respectively. Here $N_{\rm det}(\mathcal{P}_{\rm a}, \mathcal{S}_{\rm a})$ is the number of detected planets with parameters $\mathcal{P}_{\rm a}, \mathcal{S}_{\rm a}$, per unit $\mathcal{P}_{\rm a}$ and $\mathcal{S}_{\rm a}$. The quantity $N_{\rm s,a}(\mathcal{P}_{\rm a}, \mathcal{S}_{\rm a})$ is the number of unresolved point-sources on the sky the appear to be searchable.

There are many potential pitfalls. Some genuine transit signals can be missed by the detection pipeline. Some apparent transit signals are spurious, from noise fluctuations, failures of 'detrending', or instrumental effects. Stars and planets can be misclassified due to statistical and systematic errors in the measurements of their properties. Poor angular resolution causes false positives due to blends with background eclipsing binaries. *Et cetera.*

Here we focus on problems that arise from the fact that many stars exist in multiple star systems. For simplicity, we consider only binaries, and we assume that they are all spatially unresolved.

An immediate complication is that, due to dynamical stability or some aspect of planet formation, the occurrence rate of planets might differ between binary and single-star systems. If "occurrence rate" is defined as the mean number of planets within set radius and period bounds per star in a given mass interval, it must implicitly marginalize over stellar multiplicity. This means marginalizing over "occurrence rates in single star systems", "occurrence rates about primaries", and "occurrence rates about secondaries" (see Wang et al. 2015a).

Outside of astrophysical differences, there are observational biases for every term in Eq. 1. There are errors in $N_{\rm det}$ due to planet radius misclassification. There are errors in $N_{\rm s,a}$ because a given point on the sky There are errors in $p_{\rm tra}(\mathcal{P}_{\rm a}, \mathcal{S}_{\rm a})$ because stars in binaries may have different masses and radii than assumed in the single-star case. Binarity might also affect the observers' ability to correctly select searchable stars (but see Sec. 3.1 for discussion of why this is a second-order effect).

Finally, there are errors in $p_{\rm det}$ because detection efficiencies for planets orbiting single stars, primaries, and secondaries are all different.

Correcting for binarity's observational biases is non-trivial. For instance, in counting the number of selected stars, even after realizing that binaries count as two stars, one must note that the multiplicity fraction of *selected* stars is greater than that of a

volume limited sample. This is the familiar Malmquist bias: binaries are selected out to larger distances than single stars because they are more luminous. As a separate challenge, finding the correct number of detected planets in a radius bin, $N_{\rm det}$, requires knowledge of the true planetary radii. Observers deduce apparent radii. In binaries, the apparent and true radii differ because of diluting flux, and possibly because the planet is assumed to orbit the wrong star (*e.g.*, Furlan et al. 2017).

To gain intuition for the many observational biases at play, we consider a set of idealized transit surveys:

- Model #1: fixed stars, fixed planets, twin binaries;
- Model #2: fixed planets and primaries, varying secondaries;
- Model #3: fixed primaries, varying planets and secondaries.

We define our terminology in Sec. 2, and present our transit survey models in Secs. 3.1-3.3, where each subsection corresponds to a model listed above. We interpret these calculations throughout, and in Sec. 4 connect them to topical questions in the interpretation of transit survey occurrence rates. In particular, we mention the "hot Jupiter rate discrepancy", the relevance towards measurements of $\eta_\oplus$, and the implications for detailed study of Fulton et al. (2017)'s recently discovered "valley". We conclude in Sec. 5

2. DEFINITIONS

We define the occurrence rate density, Γ, as the expected number of planets per star per bin of planetary or stellar phase space. Since we will mainly be concerned with the rate density's dependence on planetary radii r, we write

$$\Gamma(r) = \frac{{\rm d}\Lambda}{{\rm d}r}, \tag{2}$$

where Λ is the occurrence rate. In this notation, "the occurrence rate of planets of a particular size" translates to an integral of Eq. 2, evaluated over a radius interval.

The above definition implicitly marginalizes the rate density over stellar multiplicity. In this study we only consider single and binary star systems. For a selected population of stars and planets, the rate density is then a weighted sum of rate densities for each system type:

$$N_{\rm tot}\Gamma(r) = N_0\Gamma_0(r) + N_1\Gamma_1(r) + N_2\Gamma_2(r), \tag{3}$$

where $i = 0$ corresponds to single stars, $i = 1$ to primaries of binaries, and $i = 2$ to secondaries of binaries. $N_{\rm tot} = \sum_i N_i$ is the total number of selected stars, and N_0, N_1, N_2 are the number of selected single stars, primaries, and secondaries. Since each selected binary system contributes both a primary and secondary star, $N_1 = N_2$. This redundancy in our notation will later prove its use.

Finally, it is helpful to write $\Gamma_i(r)$, the rate density for each type of star, as the product of a shape function and a constant:

$$\Gamma_i(r) = \frac{\mathrm{d}\Lambda_i}{\mathrm{d}r} = Z_i p_i(r), \quad \text{for } i \in \{0, 1, 2\}. \tag{4}$$

The shape function is normalized to unity. The Z_i's can be interpreted as each system type's occurrence rate Λ_i, integrated over all planetary radii. They are equivalent to the number of planets per single star, primary, or secondary.

3. IDEALIZED MODELS OF TRANSIT SURVEYS

3.1. *Model #1: fixed stars, fixed planets, twin binaries*

Since the effects of binarity are most pronounced when the two components are similar, we begin by considering a universe in which all planets are identical, and all stars are identical except that some fraction of them exist in binaries.

Expressed mathematically, from Eqs. 3 and 4 the occurrence rate density at a planet radius r can be written

$$\Gamma(r) = \delta(r_p) \times \frac{N_0 Z_0 + N_1 Z_1 + N_2 Z_2}{N_{\mathrm{tot}}}, \tag{5}$$

where $\delta(r_p)$ is the Dirac delta function, zero except at the true planet radius, r_p. The occurrence rate over any interval that includes r_p is then

$$\Lambda|_{r_p} = \frac{N_0 Z_0 + N_1 Z_1 + N_2 Z_2}{N_{\mathrm{tot}}}, \tag{6}$$

and the rate is zero over intervals that do not include r_p.

We return to our group of binarity-ignoring astronomers. They do not know the true rate density – they would like to discover it! In their signal-to-noise limited transit survey, they select stars that they think can yield transit detections. Since the noise is Poissonian, they assume

$$\frac{\text{signal}}{\text{noise}} \propto \frac{(r/R)^2}{F^{-1/2}} \propto F^{1/2} \propto L_{\mathrm{sys}}^{1/2} d^{-1}, \quad \text{(incorrectly assumed)} \tag{7}$$

for R the constant stellar radius, F the photon flux, L_{sys} the luminosity of a system, and d its distance from us. At fixed planet radius, semimajor axis, stellar radius, and stellar luminosity, a constant signal-to-noise floor yields a maximum detectable distance (Pepper et al. 2003; Pepper & Gaudi 2005). The maximum distance out to which our binarity-ignoring astronomers select stars, d_{sel}, thus scales as $L_{\mathrm{sys}}^{1/2}$.

The single stars have luminosity L_1, and the twin binaries have luminosity $2L_1$. Thus the twin binaries are selected out to a distance $\sqrt{2}$ times that of single stars. This is a bad move, because the transit signal for any planet in a twin binary will be diluted by a factor of two:

$$\frac{\text{signal}}{\text{noise}} \propto \frac{\mathcal{D}(r/R)^2}{F^{-1/2}} \propto \mathcal{D} F^{1/2} \propto \mathcal{D} L_{\mathrm{sys}}^{1/2} d^{-1}, \quad \text{(true)} \tag{8}$$

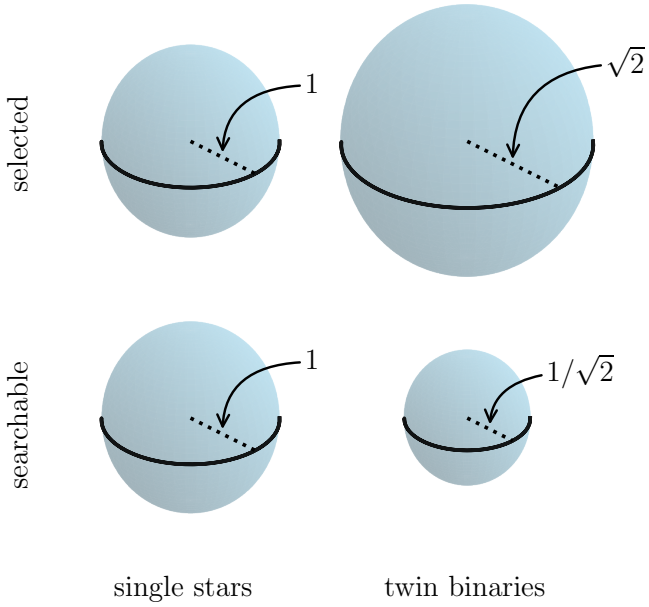

Figure 1. Cartoon of the different selected and searchable volumes for single stars (left column), and twin binaries (right column). This model (#1) assumes all stars have equal mass and luminosity. Since the observer does not recognize the brighter binaries, they select them out to a larger distance, $\sqrt{2}\times$ that of single stars. However, dilution causes the twin binaries to only be searchable in one eighth of their selected volume.

where the dilution is $\mathcal{D} \equiv L_{\rm host}/L_{\rm sys}$, for $L_{\rm host}$ the the planet host's luminosity. This means that the true maximum searchable distance for binaries, $d_{\rm det}$, is $1/\sqrt{2}$ times that of single stars. The situation is illustrated in Fig. 1: only one in eight selected stars in binaries are truly searchable.

What do the observers ignoring binarity infer?—The binarity-ignoring observers assume that all points on the sky with flux above some minimum are searchable. They correct their assumed number of searchable stars for the transit probability. As a function of apparent radius, they then report an apparent rate density of

$$\Gamma_a(r_a) = \delta(r_p) Z_0 \frac{N_0}{N_0 + N_1} + \delta\left(\frac{r_p}{\sqrt{2}}\right)(Z_1 p_{\rm det,1} + Z_2 p_{\rm det,2}) \frac{N_1}{N_0 + N_1}, \tag{9}$$

where $p_{\rm det,1}$ ($p_{\rm det,2}$) is the probability that a selected primary (secondary) is searchable. In this example, $p_{\rm det,1} = p_{\rm det,2} = 1/8$; the detection efficiency is the ratio of the searchable to selected volumes.

The true rate density (Eq. 5) and the apparent rate density (Eq. 9) differ in that

1. The total number of selected stars, $N_{\rm tot} = N_0 + N_1 + N_2$, was miscounted.
2. The detection efficiency was incorrectly assumed to be 1 for all selected stars. In reality, only one in eight binaries were searchable.

3. The inferred radii in binary systems are all $\sqrt{2}$ too small.

To assess the severity of these errors, we need to make assumptions about the stellar and planetary populations. The important quantity for the stellar population is N_1/N_0, the ratio of selected primaries (or binaries) to singles. We can define

$$\mu \equiv \frac{N_1}{N_0} = \frac{n_b}{n_s}\left(\frac{d_{\rm sel,b}}{d_{\rm sel,s}}\right)^3 = \frac{\rm BF}{1-\rm BF}(1+\ell)^{3/2}, \tag{10}$$

where n_b and n_s are the number density of binaries and singles in a volume limited sample, and the maximum selected distance for binary and single systems are $d_{\rm sel,b}$ and $d_{\rm sel,s}$. The light ratio ℓ is defined relative to the primary, so that $L_{\rm sys} = L_1(1+\ell)$. The binary fraction in a volume limited sample is "BF". For instance, Raghavan et al. (2010) found a multiplicity fraction[1] of 0.44 for primaries with masses from $0.7M_\odot$ to $1.3M_\odot$. "Twin binaries" are perhaps 10-20% of the binaries in a volume-limited sample, depending on how "twin" is defined. Thus a representative twin binary fraction for this model is BF $\approx$ 0.05-0.1.

Further, we need to assume knowledge of the true number of planets per single, primary, and secondary star (Z_0, Z_1, and Z_2). Taking $Z_0 = Z_1 = Z_2 = 1/2$, we plot the resulting occurrence rates as a function of planet radius in Fig. 2. Though it is impossible for an observer to isolate any one of binarity's biases without also addressing the others, mathematically it is simply a matter of modifying the appropriate terms in Eq. 9. The resulting rates are also shown in Fig. 2, and demonstrate how each error individually affects the overall inferred rate.

Correction to inferred rate density and inferred rate—We define a rate density correction factor, X_Γ, as the ratio of the apparent to true rate densities:

$$X_\Gamma \equiv \frac{\Gamma_a}{\Gamma}. \tag{11}$$

This correction factor can be a function of whatever parameters Γ_a and Γ depend on; in this study, the planet radius is most relevant.

If we continue assuming that the number of planets per single, primary, and secondary star are equal ($Z_0 = Z_1 = Z_2$), we find a rate density correction factor at the true planet radius of

$$X_\Gamma(r_p) = \frac{1}{1+\mu}, \tag{12}$$

This yields a correction of 0.76 if BF = 0.1, and 0.87 if BF = 0.05. Rephrasing the result, if the twin binary fraction were $(2^{3/2}+1)^{-1} \approx 0.26$, then the apparent rate would be half the true rate. Fortunately, in most contexts the twin binary fraction is not that high.

[1] The binary fraction is the fraction of systems in a volume-limited sample that are binary. It is equivalent to the multiplicity fraction if there are no triple, quadruple, or higher order multiples. In that case, BF $= n_b/(n_s+n_b)$.

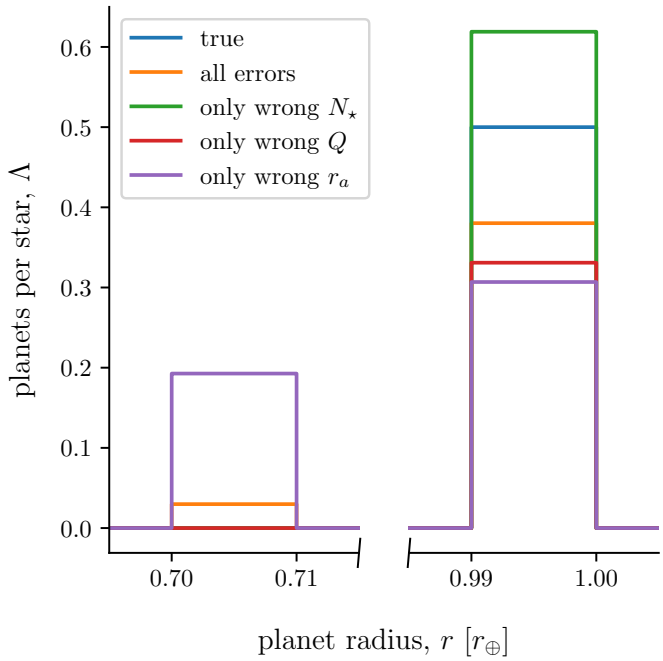

Figure 2. Inferred planet occurrence rates over $0.01 r_\oplus$ bins in planet radius, for Model #1. This model has fixed stars, fixed planets, and twin binaries. It assumes a twin binary fraction of BF = 0.1. If the true planet radius is r_p, all planets detected in binaries will have apparent radii $r_a = r_p/\sqrt{2}$. We illustrate the individual biases by separating them. On this and future plots, "only wrong $N_\star$" means the only error is an incorrectly assumed number of selected stars; "only wrong Q" means the only error is an incorrectly assumed completeness (including both miscalculated $p_{\rm tra}$ and fraction of selected stars that are searchable, $p_{\rm det}$); "only wrong r_a" means the only error is in miscalculated planetary radii, due to both transit depth dilution and also wrongly assumed host star radii.

An alternative assumption is that secondaries do not host planets. In that case, $Z_0 = Z_1$, and $Z_2 = 0$. The correction to the rate density at the true planet radius becomes

$$X_\Gamma(r_p) = \frac{1+2\mu}{(1+\mu)^2}. \tag{13}$$

This evaluates to 0.94 if BF = 0.1, and 0.98 if BF = 0.05. While it is hard to justify the assumption that secondaries are planet-less, it is worth noting that Γ_a/Γ is sensitive to the relative number of planets per single, primary, and secondary.

3.2. *Model #2: fixed planets and primaries, varying secondaries*

Our binary-twin model provides a simple estimate of binarity's systematic effects, but perhaps it is too simple. We begin introducing realism by first letting the light ratio $\ell = L_2/L_1$ vary across the binary population. It does so because the underlying mass ratio $q = M_2/M_1$ varies. We keep the primary mass fixed as M_1, which is also the mass of all single stars.

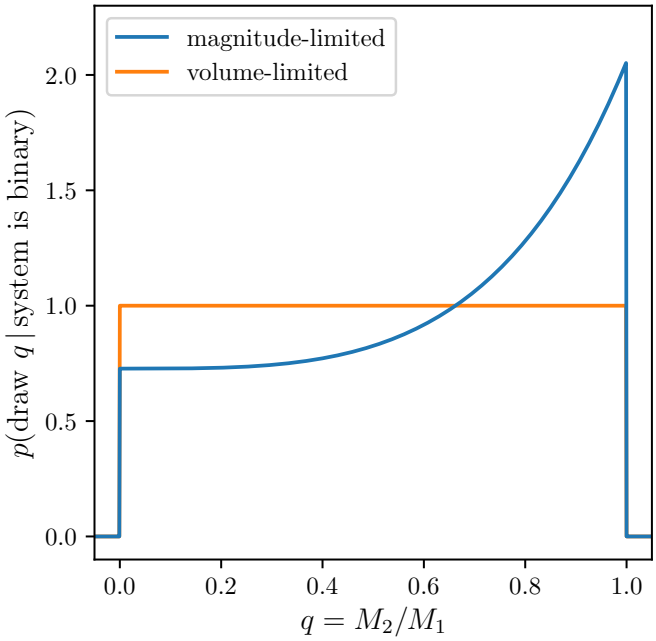

Figure 3. The mass ratio distribution for a magnitude-limited sample of binary stars, in which the underlying volume-limited distribution is uniform (qualitatively similar to *e.g.*, Raghavan et al. (2010)'s Fig. 16). The entire bias can be understood analytically (Eq. 15).

We parametrize the distribution of binary mass ratios in a volume-limited sample as a power law: $p(q) \propto q^{\beta}$. For binaries with solar-type primaries[2], β is probably between 0 and 0.3. We further assume that stars are a one-parameter family, $R \propto M \propto L^{1/\alpha}$, so that a drawn value of q determines everything about a secondary.

The rate density in this model, $\Gamma(r, q)$, is the sum of the rate densities for each system type:

$$\Gamma(r, q) = \delta(r_p) \times \frac{N_0 Z_0 + N_1 Z_1 + N_2 Z_2 p_2(q)}{N_{\rm tot}} \tag{14}$$

where $p_2(q)$ is mass-ratio dependent shape function in secondaries. A fully general approach would parametrize $p_2(q)$ as a power law, $p_2(q) \propto q^{\gamma}$. For simplicity we will always take $\gamma = 0$, the uniform case. The interpretation of Z_i is still "the number of planets per star of type i", but now for secondaries this must include a marginalization over both the mass ratio and the planet radius.

There is also a Malmquist bias in Eq. 14, hidden away in the numbers of selected stars. This is because the selected sample at a fixed planet radius and period is magnitude-limited. Given a binary, the probability of drawing a mass ratio q in a magnitude-limited sample scales as

$$p(\text{draw } q \,|\, \text{system is binary}) \propto q^{\beta}(1 + q^{\alpha})^{3/2} \tag{15}$$

[2] Duchêne & Kraus (2013), fitting all the multiple systems of Raghavan et al. (2010)'s Fig 16, find $\beta = 0.28 \pm 0.05$ for $0.7 < M_{\star}/M_{\odot} < 1.3$. Examining only the binary systems of Raghavan et al.'s Fig 16, the distribution seems (by eye) to be roughly uniform, $\beta \approx 0$, except for an excess of twin binaries with $q \approx 1$, and an obvious lack of $q < 0.1$ stellar companions.

where q^β is the volume-limited probability of drawing a binary of mass ratio q, and the latter term is the Malmquist bias. We show the magnitude-limited mass ratio distribution for the $\beta = 0$ case in Fig. 3. We emphasize that in Monte Carlo simulations of transit surveys, it is important to draw binaries from the correctly biased mass-ratio distribution (*e.g.*, Bakos et al. 2013; Sullivan et al. 2015; Günther et al. 2017).

The occurrence rate corresponding to Eq. 14's rate density for specific mass ratios of interest $q_{\rm min} < q < q_{\rm max}$ is then

$$\Lambda|_{r_p,q_{\rm min},q_{\rm max}} = \frac{N_0 Z_0 + N_1 Z_1 + N_2 Z_2 f_2}{N_{\rm tot}}, \tag{16}$$

for

$$f_2 \equiv \int_{q_{\rm min}}^{q_{\rm max}} p_2(q)\,{\rm d}q, \tag{17}$$

where $p_2(q) \propto q^\gamma$, and is normalized to unity.

What do the observers ignoring binarity infer?—As a reminder, the binary-ignoring observers compute an apparent rate density by correcting the number of detections per star for the transit probability and the detection efficiency. In this process, they make the following errors:

1. They assume that they have selected $N_0 + N_1$ stars, while they have actually selected $N_0 + N_1 + N_2$.

2. They assume that every star within the maximum selected distance is searchable. This is true for single stars. For binaries, the actual detection efficiency is the ratio of the number of searchable stars to the number of selected stars. For primaries,

$$p_{\rm det,1} = \left(\frac{d_{\rm det,1}}{d_{\rm sel}}\right)^3 = \mathcal{D}_1^3 = (1+q^\alpha)^{-3}, \tag{18}$$

   where we have assumed that all single stars and primaries have the same properties, and have used $\ell = q^\alpha$. For secondaries,

$$p_{\rm det,2} = \left(\frac{d_{\rm det,2}}{d_{\rm sel}}\right)^3 = \mathcal{D}_2^3 \left(\frac{R_1}{R_2}\right)^6 \left(\frac{T_{\rm dur,2}}{T_{\rm dur,1}}\right)^{3/2} = (1+q^{-\alpha})^{-3} q^{-5}, \tag{19}$$

   where subscripts '1' and '2' correspond to primaries and secondaries, and we used the scaling relation $T_{\rm dur} \propto \rho_\star^{-1/3} \propto R_\star^{2/3}$.

3. They assume a transit probability for all stars of $p_{\rm tra} = R_\star/a$. For planets orbiting secondaries at fixed period, the true transit probability is $q^{2/3} p_{\rm tra}$, since the secondaries have smaller radii and masses.

4. The true planetary radii r are interpreted as apparent radii r_a. In binaries, the apparent radii depend on whether the host is the primary or secondary:

$$r_a = \begin{cases} r_p(1+q^{\alpha})^{-1/2} & \text{for } i=1, \text{ primary} \\ r_p(1+q^{-\alpha})^{-1/2}q^{-1}, & \text{for } i=2, \text{ secondary.} \end{cases} \tag{20}$$

The factor of q^{-1} for the secondary case accounts for the observer assuming all transit signals come from stars of fixed size.

To write the apparent rate density as a function of the apparent radius r_a, we marginalize out the planet period, semimajor axis, and stellar radius (or equivalently the mass ratio, for binaries):

$$\Gamma_a(r_a) = \frac{N_0}{N_0+N_1} Z_0 \delta(r_p) + \frac{N_1}{N_0+N_1} \left(Z_1 I_1(r_a) + Z_2 I_2(r_a)\right). \tag{21}$$

The ratio of primaries to singles, $\mu = N_1/N_0$, is now less than that of Model #1 (cf. Eq. 10). This is because a distribution of light ratios ℓ leads to a distribution of maximum selected distances. Integrating over the mass ratios from $q = 0$ to 1, one finds a dimensionless integral

$$\mu \equiv \frac{N_1}{N_0} = \frac{\mathrm{BF}}{1-\mathrm{BF}} \left(2^{3/2} - \int_1^{\sqrt{2}} u^2(u^2-1)^{1/\alpha}\,\mathrm{d}u\right). \tag{22}$$

Given a binary fraction, Eq. 22 fully specifies the "weights" in Eq. 21. The $I_1(r_a)$ and $I_2(r_a)$ terms are found by marginalizing over the joint distribution of apparent radius and mass ratio:

$$I_i(r_a) = \int_0^1 p(\text{has detected planet}, r_a, q | \text{star is type } i)\,\mathrm{d}q, \quad \text{for } i \in \{1,2\}, \tag{23}$$

$$= \int_0^1 p(\text{has detected planet} | r_a, q, \text{star is type } i) \times p(r_a | q, \text{star is type } i)\, p(q | \text{star is type } i)\,\mathrm{d}q. \tag{24}$$

The first term is the detection efficiency; the second is a δ-function of the apparent radius; the last is the mass ratio distribution given by Eq. 15. An analytic solution can be found for $i = 1$. For $i = 2$ there is no analytic solution, because evaluating the integral requires imposing the constraint that $r_a = r_p(1+q^{-\alpha})^{-1/2}q^{-1}$. This equation can be re-written

$$\left(\frac{r_p}{r_a}\right)^2 = q^2 + q^{-\alpha+2}, \tag{25}$$

which has no analytic solution for $q(r_a)$ except for special values of α, the mass-luminosity exponent. For $\alpha = 3.5$, our nominal case, semianalytic solutions do exist. However, since our main interest is in understanding the qualitative behavior of the solutions, we derive a limiting case, and then proceed numerically.

Limiting case of rate density correction—Recall that the rate density correction factor, X_Γ, is the ratio of the apparent to true rate densities. We consider a "nominal model" in which the stellar population is similar to Sun-like stars in the local neighborhood: BF = 0.44, $\alpha = 3.5$, $\beta = 0$. Our default assumption is also that the occurrence of planets is independent of stellar mass ($\gamma = 0$), so secondaries have the same occurrence rate as primaries and single stars. Under these assumptions, the true rate density is

$$\Gamma(r) \approx \delta(r_p) \left(Z_0 + Z_1 + Z_2\right)/3, \tag{26}$$

where the coefficients of 1/3 are accurate to within one percent of the true coefficients. Ignoring binarity, the observer finds an apparent rate density

$$\Gamma_a(r) = c_0 Z_0 \delta(r_p) + c_1 Z_1 I_1(r_a) + c_2 Z_2 I_2(r_a), \tag{27}$$

for $c_0 \approx 0.49$, and the coefficients c_1, c_2 unknown. We can evaluate the correction term at $r = r_p$, since $\lim_{r_a \to r_p} I_i(r_a) = 0$ for $i \in \{1, 2\}$:

$$X_\Gamma(r = r_p) \approx \frac{3 c_0 \Lambda_0}{\Lambda_0 + \Lambda_1 + \Lambda_2}. \tag{28}$$

If all the Z_i's are equal, $X_\Gamma(r = r_p) \approx 0.49$. If there are no planets around the secondaries, $X_\Gamma(r = r_p) \approx 0.74$.

Numerical approach—To maintain simplicity, we develop a Monte Carlo program to simulate our toy transit surveys. The program generates a stellar population, assigns planets to the stars, and then calculates which planets are detectable. It then computes the apparent and true planet occurrence rates as a function of planet radius. We discuss the details below, and refer the interested reader to our online implementation[3].

First, the user must specify the free parameters that describe the stellar and planetary population. These values include the binary fraction, and the true planet occurrence rates around single stars, primaries, and secondaries (the Z_i's; recall Eq. 4). There is also an arbitrary absolute number of selected stars.

Once the user specifies the free parameters, the program constructs a population of selected stars. Each selected star is assigned a type (single, primary, secondary), a binary mass ratio (if it is not single), and the property of whether it is "searchable". The relative number of binaries to primaries is set by Eq. 22. The mass ratios are drawn from the appropriate magnitude-limited distribution (Eq. 15). If it is single, a selected star is assumed to be searchable. If it is a primary or secondary, its searchability is determined by a uniform draw from either Eq. 18 or Eq. 19, as appropriate.

Assigning planets, each selected star receives a planet at the rate Z_i, according to its type. The radii of planets are assigned independently of any host system

[3] https://github.com/lgbouma/binary_biases

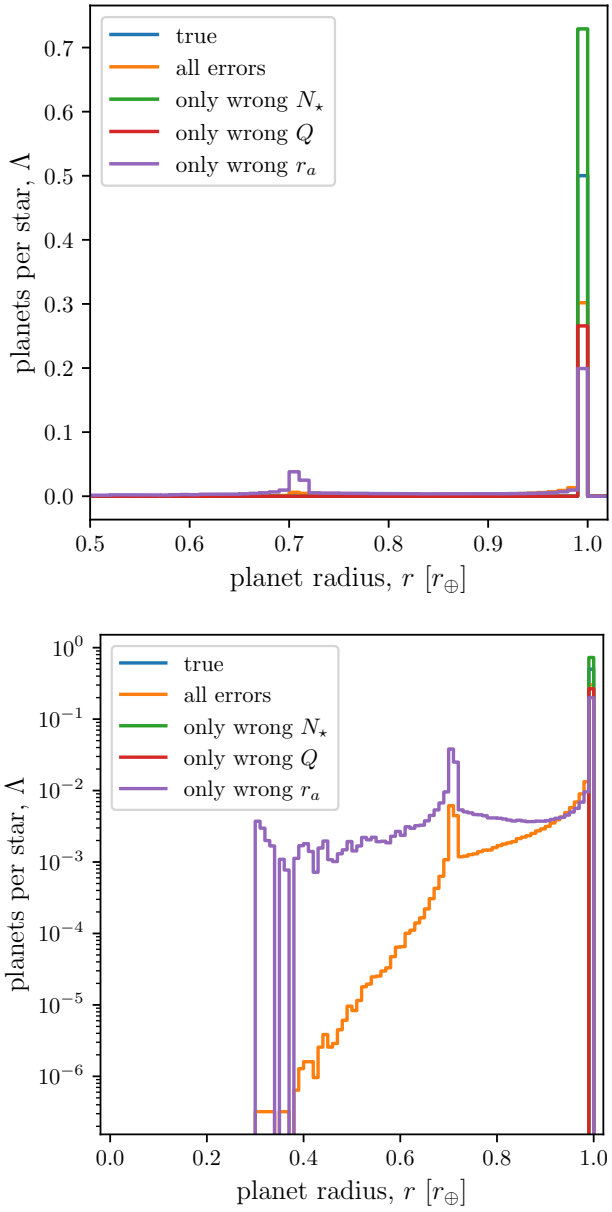

Figure 4. Inferred planet occurrence rates as a function of planet radius in Model #2 (*top:* linear, *bottom:* logarithmic). This model has fixed planets and primaries, and varying secondary masses, radii, and luminosities. The latter three lines are described in Fig. 2.

property, and can be sampled for an arbitrary distribution (*e.g.*, power law; delta function). The absolute transit probability, $p_{\rm tra}$ is set arbitrarily, and the probability of a planet transiting a secondary is set as $q^{2/3} \times p_{\rm tra}$. A planet is "detected" when a) it transits, and b) its host star is searchable. For detected planets, apparent radii are computed according to analytic formulae that account for both dilution and the misclassification of stellar radii (Eq. 20). We assume that the observers think that all transits are around single stars.

We then compute rates in bins of true planet radius and apparent planet radius. In a given radius bin, the true rate is found by counting the number of planets that exist around selected stars of all types (singles, primaries, secondaries), and dividing by the total number of these stars. The apparent rates are found by counting the number of detected planets that were found in an apparent radius bin, dividing by the geometric transit probability for single stars, and dividing by the apparent total number of stars.

Numerical results for Model #2—We first validate our model by ensuring it produces the analytically-predicted results for Model #1, and the limiting case of Model #2 described above. Following validation, we assume BF = 0.44, $\alpha = 3.5$, $\beta = \gamma = 0$, and take $Z_0 = Z_1 = Z_2 = 0.5$. We then compute the true and apparent occurrence rates over bins in planet radius. The results are shown in Fig. 4. Evidently, dilution produces a spectrum of apparent planetary radii. This leads to overestimated rates everywhere except where at the true planet radius, where the rate is underestimated by a factor of two. Compared to Model #1 (Fig. 2), the general picture is that the apparent radius distribution is "blurred" by the varying secondary light ratios.

3.3. *Model #3: Fixed primaries, varying planets and secondaries*

As in the previous model, all single and primary stars in this model have identical properties. The secondaries have masses, radii, and luminosities that vary between systems: $M \propto R \propto L^{1/\alpha}$. The only addition is that we now let the radii of planets vary: they are assigned independently of any host system property, and are sampled from the true radius distribution, which we take as

$$p_r(r) \propto \begin{cases} r^{\delta} & \text{for } r \geq 2r_{\oplus} \\ \text{constant} & \text{for } r \leq 2r_{\oplus}. \end{cases} \tag{29}$$

Following Howard et al. (2012)'s measurement, we take $\delta = -2.92$. Our "nominal model" remains the same: the binary fraction is 0.44, $\alpha = 3.5$, $\beta = \gamma = 0$. We take Z_i, the number of planets per single, primary, and secondary, to be equal.

For this model, we forgo analytic development and simply run our Monte Carlo program[4]. The resulting occurrence rates are shown in Fig. 5. For the assumed planetary and stellar distributions, the inferred rate is underestimated over all radii.

Hot Jupiter occurrence rates—Taking Fig. 5 and counting the number of planets per star with $r > 8r_{\oplus}$, we can compare the true and inferred hot Jupiter occurrence rates. Under the above assumptions, the true rate is 9.1 hot Jupiters per thousand stars. The inferred rate is 6.9 per thousand stars. This means that the inferred rate underestimates the true rate by a multiplicative factor of $\sim$1.3.

[4] One might worry that our Monte Carlo program does not increase the number of selected stars as the square of the planet radius (Eq. 8). We can omit this dependence because in our model N_1/N_0 is independent of desired planet radius, and all other terms in the rate densities (*e.g.*, Eqs. 14 and 21) are independent of the number of selected stars.

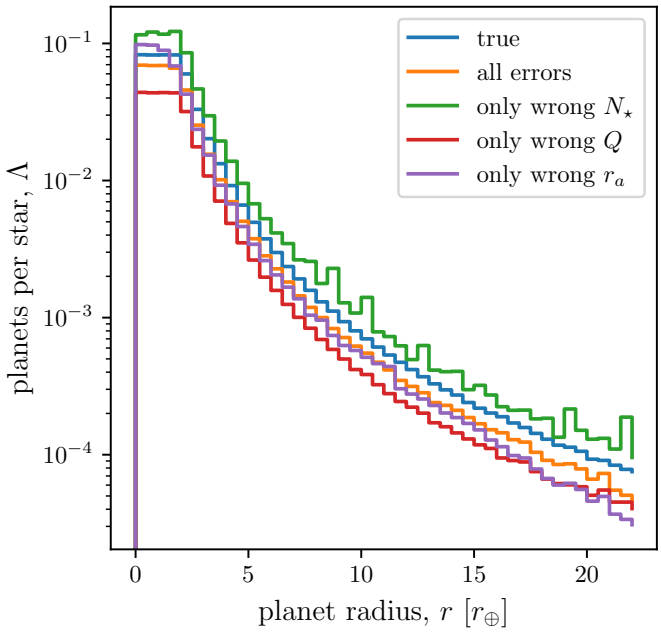

Figure 5. Inferred planet occurrence rates as a function of planet radius in Model #3. This model has fixed primaries and single stars, but varying secondaries. The true planet radius distribution is a power law with exponent -2.92 above $2r_\oplus$, below which it is uniform (similar to Howard et al. 2012).

However, this result only applies under the assumption that $Z_0 = Z_1 = Z_2$. If hot Jupiters are less common around lower mass stars, it would be more sensible to consider $Z_2 < Z_0$, while letting single stars and primaries host planets at the same rate. Therefore in Fig. 6 we let Z_2 vary, and show the resulting inferred and true hot Jupiter ($r > 8r_\oplus$) rates. The result is that the inferred rate is nearly independent of Z_2 – this is because most ($< 1/10$) secondaries are not searchable, and so their completeness fraction is much smaller than that of primaries or single stars. This means far fewer detected hot Jupiters orbit secondaries, and so they hardly affect the inferred rate. While the "true rate" across the entire population is linearly dependent on Z_2, the rate around singles and primaries (Fig. 6 green line) is independent of that around secondaries.

The rate of Earth analogs—This model provides an estimate of the apparent and true rates as a function of radius (Fig. 5). At Earth's radius, the result is that the inferred rate is 0.84× the true rate around single stars, assuming that the Z_i's are equal. Similar to the above case of the hot Jupiters, if we vary the true Z_2 while keeping $Z_0 = Z_1$, the ratio of the inferred to true rate around single stars changes by only a few percent (shown in Fig. 7). The ratio of the inferred to the true rate, $(\Lambda_{\rm inferred}/\Lambda)_{r=r_\oplus}$ varies substantially, but by at most 50% in the (unrealistic) limiting case that secondaries do not host planets.

4. DISCUSSION

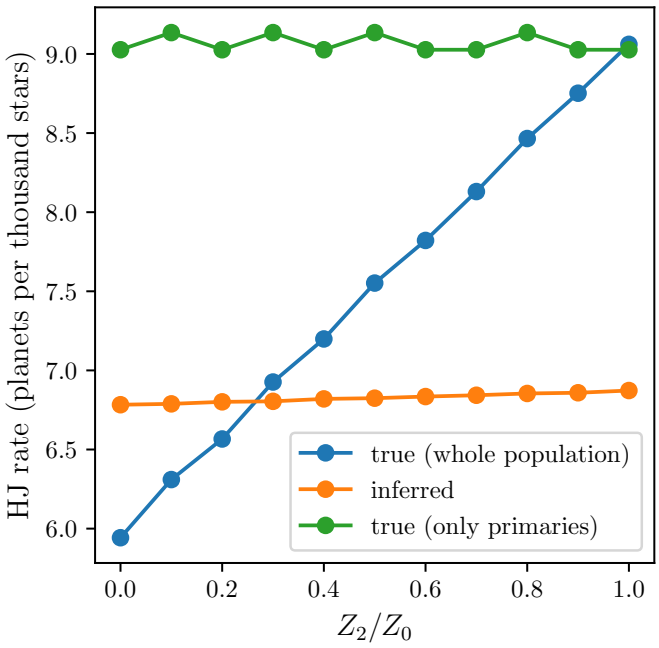

Figure 6. Z_i is the occurrence rate integrated over all possible phase space for the i^{th} system type. $Z_2/Z_0 = 1$ corresponds to an equal number of planets per secondary as per single star; $Z_2/Z_0 = 0$ corresponds to secondaries not having any planets. In our Model #3, though the true HJ occurrence rate is highly dependent on Z_2, the inferred rate hardly depends on whether secondaries have HJs. This means that the "correction factor" between the inferred rate and the true rate around single stars is underestimated by a multiplicative factor of ≈ 1.3, independent of the HJ rate around secondaries. The "HJ rate" is the summed rate from Fig. 5 above $8r_\oplus$.

How has binarity been considered in occurrence rate measurements?—Binarity introduces systematic uncertainty to star and planet counts, and also to estimates of pipeline completeness. In spite of this fact, stellar multiplicity has mostly been ignored in calculations of planet occurrence rates using transit survey data[5] (*e.g.*, Howard et al. 2012; Fressin et al. 2013; Foreman-Mackey et al. 2014; Dressing & Charbonneau 2015; Burke et al. 2015). For *Kepler* occurrence rates specifically, it seems that no one has yet carefully assessed binarity's importance, or lack thereof. While we do not resolve the problem, we do suggest the approximate scale of the necessary corrections in a survey-independent manner.

Of course, on a system-by-system level stellar multiplicity affects the interpretation of planet candidates. High resolution imaging campaigns have measured the multiplicity of almost all *Kepler* Objects of Interest (Howell et al. 2011; Adams et al. 2012, 2013; Horch et al. 2012, 2014; Lillo-Box et al. 2012, 2014; Dressing et al. 2014; Law et al. 2014; Cartier et al. 2015; Everett et al. 2015; Gilliland et al. 2015; Wang et al. 2015b,c; Baranec et al. 2016). The results of these programs have been collected by Furlan et al. (2017), and they represent an important advance in understanding the

[5] A list of occurrence rate papers is maintained at `https://exoplanetarchive.ipac.caltech.edu/docs/occurrence_rate_papers.html`

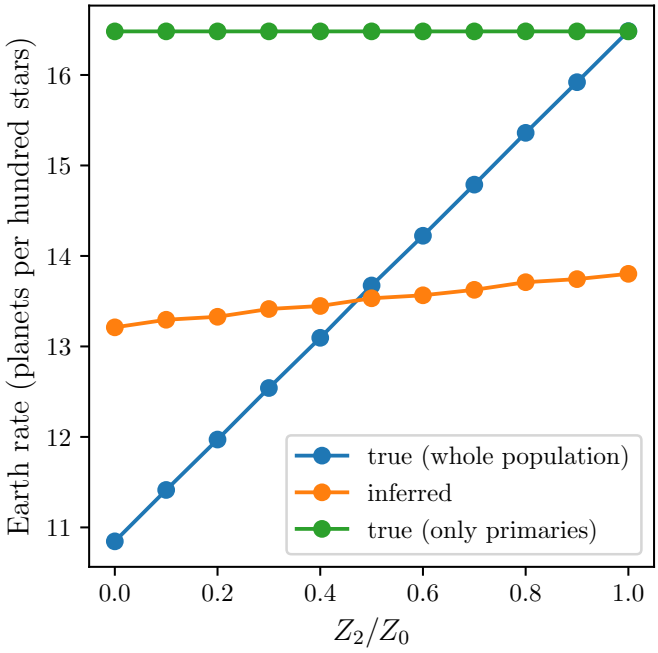

Figure 7. Same as Fig. 6, but for Earth-sized planets. The absolute values given on the y-axis found by summing the rate from Fig. 5 for planetary radii from 0.5 to $1.5r_\oplus$ (this is a toy model, and they do not reflect an actual determination of $\eta_\oplus$). The relative values show that the inferred rate for Earths is roughly independent of the occurrence rate (integrated over all radii) around secondaries. However, it is systematically lower than the true rate around single and primary stars, by $\approx 20\%$.

KOI sample's multiplicity statistics. In particular, they can be immediately applied to rectify binarity's effects on the mass-radius diagram (Furlan & Howell 2017).

The high resolution imaging campaign is also beginning to connect with occurrence rate calculations. The most recent rate studies have used Furlan et al. (2017)'s catalog to test the effects of removing KOI hosts with known companions, which helps reduce contamination in the "numerator" of the occurrence rate (Fulton et al. 2017; Petigura et al. 2018, in preparation). However, without an understanding of the multiplicity statistics of the non-KOI stars, the true completeness, and thus the true occurrence rates, will remain biased. The first-order correction that we suggest, given the impracticality of performing high-resolution imaging of every selected star in a transit survey, is to model the detection pipeline's efficiency while accounting for binarity. For *Kepler*, this would require high resolution imaging of a comparison sample of non-KOI host stars. If the associated multiplicity statistics are then included in a model of the pipeline's detection efficiency, and the number of selected stars is appropriately counted, it would correct most of binarity's biases.

The hot Jupiter rate discrepancy—There is at least one context in which ignoring binarity may already be leading to discrepant measurements. Hot Jupiter occurrence rates measured by transit surveys ($\approx 0.5\%$) are marginally lower than those found by radial velocity surveys ($\approx 1\%$; see Table 1). Though the discrepancy has weak statistical

significance ($< 3\sigma$), one reason to expect a difference is that the corresponding stellar populations have distinct metallicities. As argued by Gould et al. (2006), the RV sample is biased towards metal-rich stars, which have been measured by RV surveys to preferentially host more giant planets (Santos et al. 2004; Fischer & Valenti 2005). Investigating the discrepancy from the metallicty angle, Guo et al. (2017) measured the *Kepler* field's mean metallicity to be $[\mathrm{M/H}]_{\mathrm{Kepler}} = -0.045 \pm 0.009$, which is lower than the California Planet Search's mean of $[\mathrm{M/H}]_{\mathrm{CPS}} = -0.005 \pm 0.006$. The former value agrees with that measured by Dong et al. (2014). Based on their measurements, Guo et al. then argued that the metallicity difference could account for a $\approx 20\%$ relative difference in the measured rates between the CKS and *Kepler* samples – not a factor of two. Guo et al. concluded that "other factors, such as binary contamination and imperfect stellar properties" must also be at play.

Aside from surveying stars of varying metallicities, radial velocity and transit surveys differ in how they treat binarity. Radial velocity surveys typically reject both visual and spectroscopic binaries (*e.g.*, Wright et al. 2012). Transit surveys typically observe binaries, but the question of whether they were searchable to begin with is left for later interpretation. In spectroscopic follow-up of candidate transiting planets, the prevalence of astrophysical false-positives may also lead to a bias against confirmation of transiting planets in binary systems.

Ignoring these complications, in this work we showed that binarity biases transit survey occurrence rates through its effects on completeness, star counts, and the apparent radii of detected planets. Specifically, our results from Sec. 3.3 indicate that binarity could lead to underestimated HJ rates by a multiplicative factor of ≈ 1.3.

To assess the effect this might have towards resolving the hot Jupiter rate discrepancy we ask: what is the probability of Wright et al. (2012)'s result, given a rate drawn from the stated bounds of Petigura et al. (2018, in preparation)? In other words, we first take the true HJ rate per thousand stars as $\Lambda_{\mathrm{HJ}} = 5.7 \pm 1.3$, with Gaussian uncertainties. We then draw from a Poisson distribution and compute the probability of detecting at least 10 hot Jupiters in a sample of 836 stars. Without accounting for binarity or metallicity, only 4% of RV surveys would detect at least 10 hot Jupiters. If we multiply Λ_{HJ} by 1.2 to account for Guo et al. (2017)'s measured metallicity difference between the *Kepler* field and the local solar neighborhood, 9% of RV surveys would detect at least 10 hot Jupiters. If we multiply once more by 1.3 to account for binarity's bias, we find that 23% of RV surveys would detect at least 10 hot Jupiters, and any discrepancy would be rather tenuous. We emphasize that this result is only suggestive – a true resolution of the rate discrepancy would likely require a detailed understanding of the *Kepler* field's multiplicity statistics.

The rate of Earth analogs—Per *Kepler*'s primary science objective, the rate of Earth-like planets orbiting Sun-like stars has been independently measured by Youdin (2011); Petigura et al. (2013); Dong & Zhu (2013); Foreman-Mackey et al. (2014), and Burke et al. (2015). These efforts have found that the one-year terrestrial planet

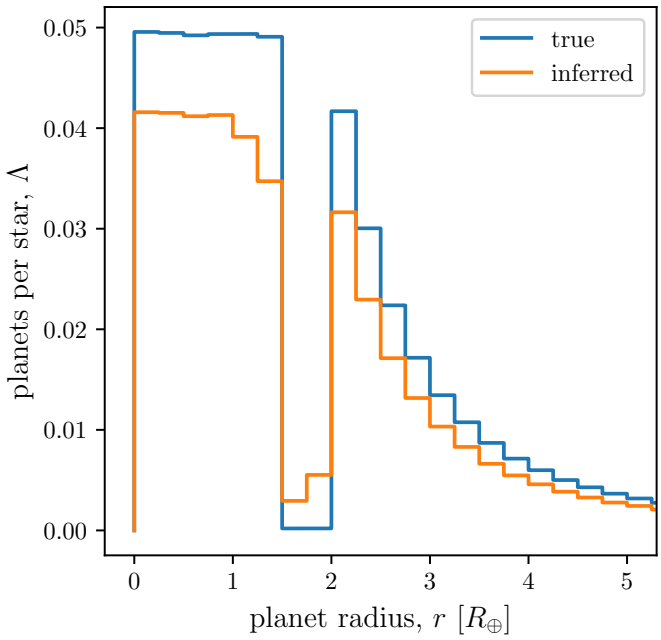

Figure 8. Inferred planet occurrence rates as a function of planet radius in a model with a radius gap (Eq. 30). Similar to Model #3, this model has fixed primaries and single stars, but varying secondaries.

occurrence rate varies between ≈ 0.03 and ≈ 1 per Sun-like star, depending on assumptions that are made when retrieving the rate (Burke et al. (2015)'s Fig. 17). In our Model #3, the inferred rate is $\approx 0.84\times$ the true rate around single stars. This bias is quite small compared to the other systematic factors that currently dominate the dispersion in $\eta_\oplus$ measurements. If a future analyses determine absolute values of $\eta_\oplus$ to better than a factor of two, binarity might merit closer attention.

One relevant caveat to our assessment of binarity's importance for $\eta_\oplus$ measurements is that none of our models included the rate density's period-dependence. However, close binaries usually provoke dynamical instabilities, leading to fewer long-period planets per star (*e.g.*, Holman & Wiegert 1999; Wang et al. 2014; Kraus et al. 2016). This effect might further bias transit survey measurements of $\eta_\oplus$ beyond our rough estimate.

Precise features of the radius valley—Using improved stellar parameters measured by the California-*Kepler* survey, Fulton et al. (2017) recently reported a "gap" in the radius-period plane (Petigura et al. 2017; Johnson et al. 2017). The existence of the gap has been independently corroborated from a sample of KOIs with asteroseismically-determined stellar parameters (Van Eylen et al. 2017). Precise measurement of the gap's features, in particular its width, depth, and shape, will require more accurate occurrence rates. To illustrate binarity's role in the issue, we make identical assumptions as in Model #3, but instead assume an intrinsic radius distri-

bution

$$p_r(r) \propto \begin{cases} r^{\delta} & \text{for } r \geq 2r_{\oplus}, \\ 0 & \text{for } 1.5r_{\oplus} < r < 2r_{\oplus}, \\ \text{constant} & \text{for } r \leq 1.5r_{\oplus}. \end{cases} \tag{30}$$

The resulting true and inferred rates are shown in Fig. 8. If left uncorrected, binarity makes the gap appear more shallow, and flattens the step-function edges. At present though, binarity seems less important than other effects that would "blur" the gap in the planet radius dimension. In particular, the valley's period-dependence is almost certainly not flat (Van Eylen et al. 2017; Owen & Wu 2017). This means that any study assessing its width, depth, etc. only in the planet radius dimension must first account for the blurring that comes from marginalizing over the periods.

Does a detected planet orbit the primary or secondary?—Ciardi et al. (2015) studied the effects of stellar multiplicity on the planet radii derived from transit surveys. They modeled the problem for *Kepler* objects of interest by matching a population of binary and tertiary companions to KOI stars, under the assumption that the KIC-listed stars were the primaries. They then computed planet radius correction factors assuming that *Kepler*-detected planets orbited the primary or companion stars with equal probability (their Sec. 5). Under these assumptions, they found that any given planet's radius is on average underestimated by a multiplicative factor of 1.5.

Our models show that assuming a detected planet has equal probability of orbiting the primary or secondary leads to an overestimate of binarity's population-level effects. A planet orbiting the secondary does lead to extreme corrections, but these cases are rare outliers, because the searchable volume for secondaries is so much smaller than that for primaries. Phrased in terms of the completeness, in our Model #3 only $\sim 6\%$ of selected secondaries are searchable, compared to $\sim 60\%$ of selected primaries. This means that when high-resolution imaging discovers a binary companion in a system that hosts a detected transiting planet, the planet is much more likely to orbit the primary. This statement is independent of the fact that planets are often confirmed to orbit the primary by inferring the stellar density from the transit duration.

On the utility for future occurrence rate measurements—*TESS* is expected to discover over 10^4 giant planets (Sullivan et al. 2015). Though they will be difficult to distinguish from false positives, one possible use of this overwhelmingly large sample will to measure an occurrence rate of short-period giant planets. Our work indicates that if this measurement is to be more accurate than $\sim 30\%$, binarity cannot be neglected.

Independent approaches for estimating binarity's effects—T. Barclay et al. (in preparation) have performed the exercise of taking stars selected by the *Kepler* team, pairing them with a population of secondaries, injecting a realistic distribution of planet radii,

and then comparing the inferred occurrence rates with the true ones. In their model, they find that binarity leads to an inferred rate of Earth-sized planets $\approx 10\%$ less than the true rate. In our Model #3, if all Z_i's are equal (a plausible assumption in the lack of evidence to the contrary), the underestimate is by a comparable 16%.

5. CONCLUSION

This study presented three simple models for the effects of binarity on occurrence rates measured by transit surveys. The simplest of these models (Model #1) provides an order-of-magnitude estimate of how much binarity biases occurrence rates. The most realistic of these models (Model #3) suggests that binarity does lead to underestimates in transit survey occurrence rates, but with less than 30% relative error. The model further suggests that hot Jupiter rates measured by transit surveys are biased to infer $\approx 1.3\times$ fewer hot Jupiters per star than surveys that only measure occurrence rates about single stars (*i.e..,* radial velocity surveys). It also indicates that binarity's effects on the measured rates of Earth-sized planets are far smaller than current systematic uncertainties. Though our models are simplistic, their agreement with T. Barclay's recent independent simulations indicate that they capture the essential ingredients.

Table 1. Occurrence rates of hot Jupiters (HJs) about FGK dwarfs, as measured by radial velocity and transit surveys.

Reference	HJs per thousand stars	HJ Definition
Marcy et al. (2005)	12±2	$a < 0.1$ AU; $P \lesssim 10$ day
Cumming et al. (2008)	15±6	–
Mayor et al. (2011)	8.9±3.6	–
Wright et al. (2012)	12.0±3.8	–
Gould et al. (2006)	$3.1^{+4.3}_{-1.8}$	$P < 5$ day
Bayliss & Sackett (2011)	10^{+27}_{-8}	$P < 10$ day
Howard et al. (2012)	4±1	$P < 10$ day; $r_p = 8 - 32 r_\oplus$; solar subset[a]
–	5±1	solar subset extended to $Kp < 16$
–	7.6±1.3	solar subset extended to $r_p > 5.6 r_\oplus$.
Moutou et al. (2013)	10±3	*CoRoT* average; $P \lesssim 10$ day, $r_p > 4 r_\oplus$
Petigura et al. (2018, in prep)	$5.7^{+1.4}_{-1.2}$	$r_p = 8 - 24 r_\oplus$; $P = 1 - 10$ day; CKS stars[b]
Santerne et al. (2018, in prep)	9.5±2.6	*CoRoT* galactic center
–	11.2±3.1	*CoRoT* anti-center

NOTE— The first four studies use data from radial velocity surveys; the rest are based on transit surveys. Many of these surveys selected different stellar samples. "–" denotes "same as above".

[a] Howard et al. (2012)'s "solar subset" was defined as *Kepler*-observed stars with $4100\,\mathrm{K} < T_{\rm eff} < 6100\,\mathrm{K}$, $Kp < 15$, $4.0 < \log g < 4.9$. They required signal to noise > 10 for planet detection.

[b] Petigura et al. (2018, in prep)'s planet sample includes all KOIs with $Kp < 14.2$, with a statistically insignificant number of fainter stars with HZ planets and multiple transiting planets. Their stellar sample begins with Mathur et al. (2017)'s catalog of 199991 *Kepler*-observed stars. Successive cuts are: $Kp < 14.2$ mag, $T_{\rm eff} = 4700 - 6500$ K, and $\log g = 3.9 - 5.0$ dex, leaving 33020 stars.

REFERENCES

Adams, E. R., Ciardi, D. R., Dupree, A. K., et al. 2012, The Astronomical Journal, 144, 42

Adams, E. R., Dupree, A. K., Kulesa, C., & McCarthy, D. 2013, The Astronomical Journal, 146, 9

Bakos, G. ., Csubry, Z., Penev, K., et al. 2013, PASP, 125, 154

Baranec, C., Ziegler, C., Law, N. M., et al. 2016, The Astronomical Journal, 152, 18

Bayliss, D. D. R., & Sackett, P. D. 2011, The Astrophysical Journal, 743, 103

Burke, C. J., Christiansen, J. L., Mullally, F., et al. 2015, The Astrophysical Journal, 809, 8

Cartier, K. M. S., Gilliland, R. L., Wright, J. T., & Ciardi, D. R. 2015, The Astrophysical Journal, 804, 97

Ciardi, D. R., Beichman, C. A., Horch, E. P., & Howell, S. B. 2015, The Astrophysical Journal, 805, 16

Cumming, A., Butler, R. P., Marcy, G. W., et al. 2008, Publications of the Astronomical Society of the Pacific, 120, 531

Dong, S., & Zhu, Z. 2013, The Astrophysical Journal, 778, 53

Dong, S., Zheng, Z., Zhu, Z., et al. 2014, The Astrophysical Journal Letters, 789, L3

Dressing, C. D., Adams, E. R., Dupree, A. K., Kulesa, C., & McCarthy, D. 2014, The Astronomical Journal, 148, 78

Dressing, C. D., & Charbonneau, D. 2015, ApJ, 807, 45

Duchêne, G., & Kraus, A. 2013, Annual Review of Astronomy and Astrophysics, 51, 269

Everett, M. E., Barclay, T., Ciardi, D. R., et al. 2015, The Astronomical Journal, 149, 55

Fischer, D. A., & Valenti, J. 2005, The Astrophysical Journal, 622, 1102

Foreman-Mackey, D., Hogg, D. W., & Morton, T. D. 2014, The Astrophysical Journal, 795, 64

Fressin, F., Torres, G., Charbonneau, D., et al. 2013, The Astrophysical Journal, 766, 81

Fulton, B. J., Petigura, E. A., Howard, A. W., et al. 2017, The Astronomical Journal, 154, 109

Furlan, E., & Howell, S. B. 2017, arXiv:1707.01942 [astro-ph], arXiv: 1707.01942

Furlan, E., Ciardi, D. R., Everett, M. E., et al. 2017, The Astronomical Journal, 153, 71

Gilliland, R. L., Cartier, K. M. S., Adams, E. R., et al. 2015, The Astronomical Journal, 149, 24

Gould, A., Dorsher, S., Gaudi, B. S., & Udalski, A. 2006, Acta Astronomica, 56, 1

Günther, M. N., Queloz, D., Demory, B.-O., & Bouchy, F. 2017, Monthly Notices of the Royal Astronomical Society, 465, 3379

Guo, X., Johnson, J. A., Mann, A. W., et al. 2017, The Astrophysical Journal, 838, 25

Holman, M. J., & Wiegert, P. A. 1999, The Astronomical Journal, 117, 621

Horch, E. P., Howell, S. B., Everett, M. E., & Ciardi, D. R. 2012, The Astronomical Journal, 144, 165

—. 2014, The Astrophysical Journal, 795, 60

Howard, A. W., Marcy, G. W., Bryson, S. T., et al. 2012, The Astrophysical Journal Supplement Series, 201, 15

Howell, S. B., Everett, M. E., Sherry, W., Horch, E., & Ciardi, D. R. 2011, The Astronomical Journal, 142, 19

Johnson, J. A., Petigura, E. A., Fulton, B. J., et al. 2017, arXiv:1703.10402 [astro-ph], arXiv: 1703.10402

Kraus, A. L., Ireland, M. J., Huber, D., Mann, A. W., & Dupuy, T. J. 2016, The Astronomical Journal, 152, 8

Law, N. M., Morton, T., Baranec, C., et al. 2014, The Astrophysical Journal, 791, 35

Lillo-Box, J., Barrado, D., & Bouy, H. 2012, Astronomy and Astrophysics, 546, A10

—. 2014, Astronomy and Astrophysics, 566, A103

Marcy, G., Butler, R. P., Fischer, D., et al. 2005, Progress of Theoretical Physics Supplement, 158, 24

Mathur, S., Huber, D., Batalha, N. M., et al. 2017, The Astrophysical Journal Supplement Series, 229, 30

Mayor, M., Marmier, M., Lovis, C., et al. 2011, ArXiv e-prints, 1109, arXiv:1109.2497

Moutou, C., Deleuil, M., Guillot, T., et al. 2013, Icarus, 226, 1625

Owen, J. E., & Wu, Y. 2017, arXiv:1705.10810 [astro-ph], arXiv: 1705.10810

Pepper, J., & Gaudi, B. S. 2005, The Astrophysical Journal, 631, 581

Pepper, J., Gould, A., & Depoy, D. L. 2003, Acta Astronomica, 53, 213

Petigura, E. A., Howard, A. W., & Marcy, G. W. 2013, Proceedings of the National Academy of Science, 110, 19273

Petigura, E. A., Howard, A. W., Marcy, G. W., et al. 2017, arXiv:1703.10400 [astro-ph], arXiv: 1703.10400

Raghavan, D., McAlister, H. A., Henry, T. J., et al. 2010, The Astrophysical Journal Supplement Series, 190, 1

Santos, N. C., Israelian, G., & Mayor, M. 2004, Astronomy and Astrophysics, 415, 1153

Sullivan, P. W., Winn, J. N., Berta-Thompson, Z. K., et al. 2015, The Astrophysical Journal, 809, 77

Van Eylen, V., Agentoft, C., Lundkvist, M. S., et al. 2017, arXiv:1710.05398 [astro-ph], arXiv: 1710.05398

Wang, J., Fischer, D. A., Horch, E. P., & Huang, X. 2015a, The Astrophysical Journal, 799, 229

Wang, J., Fischer, D. A., Horch, E. P., & Xie, J.-W. 2015b, The Astrophysical Journal, 806, 248

Wang, J., Fischer, D. A., Xie, J.-W., & Ciardi, D. R. 2015c, The Astrophysical Journal, 813, 130

Wang, J., Xie, J.-W., Barclay, T., & Fischer, D. A. 2014, The Astrophysical Journal, 783, 4

Wright, J. T., Marcy, G. W., Howard, A. W., et al. 2012, The Astrophysical Journal, 753, 160

Youdin, A. N. 2011, ApJ, 742, 38